

Supporting Information

A thermally reversible injectable adhesive for intestine tissue repair and anti-postoperative adhesion

Wenmo Zhang^{a,†}, Runze Zhang^{c,†}, Rong Yang^a, Yage Sun^a, Qian Zhang^a, Xuequan Feng^{b*}, Chunyan Cui^{a,d*} and Wenguang Liu^{a*}

^aSchool of Material Science and Engineering, Tianjin Key Laboratory of Composite and Functional Materials, Tianjin University, Tianjin 300350, China

^bTianjin First Center Hospital, Tianjin 300192, China

^cNHC Key Laboratory of Critical Care Medicine, Department of Neurosurgery, Binhai Hospital of Tianjin Medical University General Hospital, Tianjin 300480, China

^dState Key Laboratory of Molecular Engineering of Polymers (Fudan University)

[†]These authors contributed equally to this work

*Corresponding author (E-mail: fengxuequan@126.com, cycui@tju.edu.cn, wgliu@tju.edu.cn)

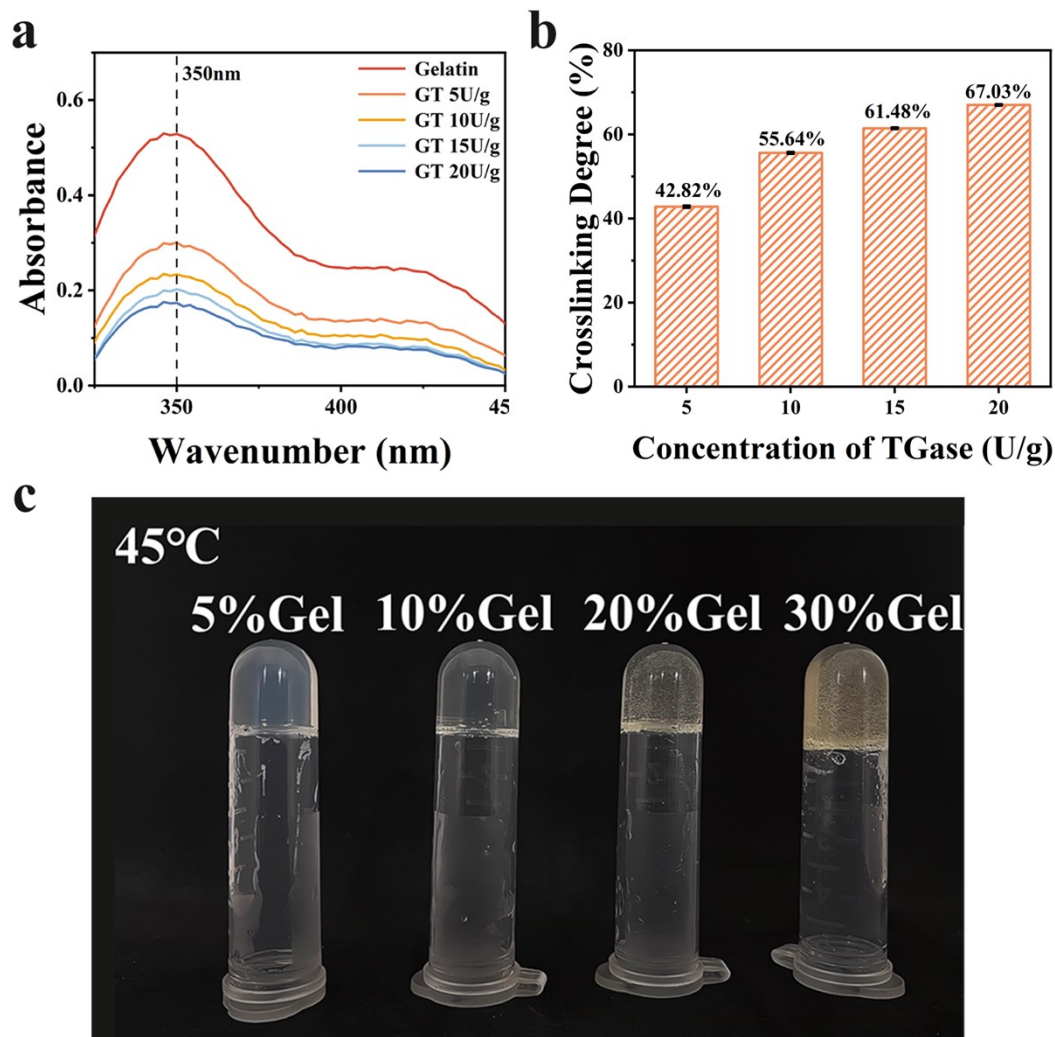


Fig. S1 (a) Absorbance of the mixed solutions of gelatin and different concentrations of TGase. (b) Calculation results of crosslinking degree of gelatin after mixed with different concentration of TGase. (c) Gelatin-TGase hydrogel with different concentration of gelatin at 45 °C.

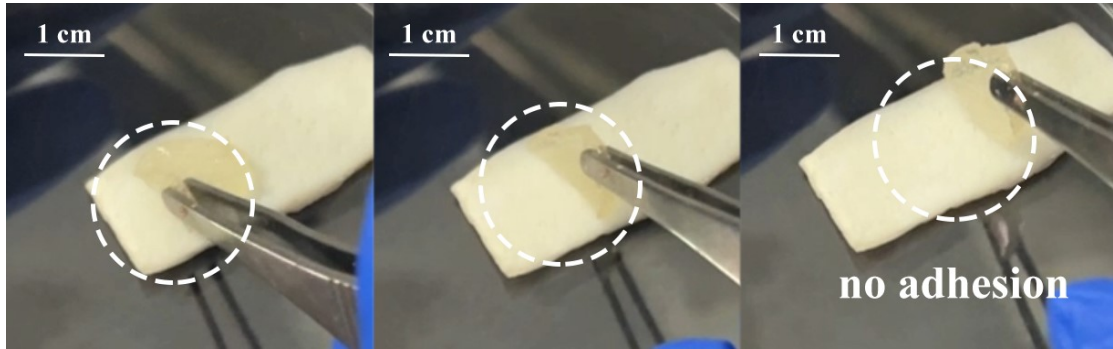


Fig. S2 Photos showing that Gelatin -TGase hydrogel has no tissue adhesion at 37 °C.

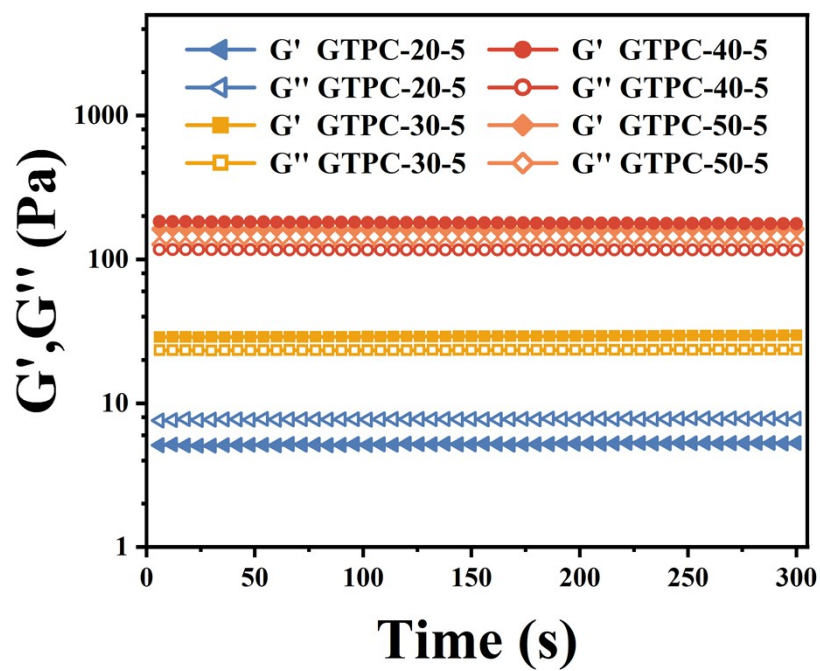


Fig. S3 Time sweep rheological analysis to evaluate stability of GTPC hydrogels with different gelatin concentration at 37 °C.

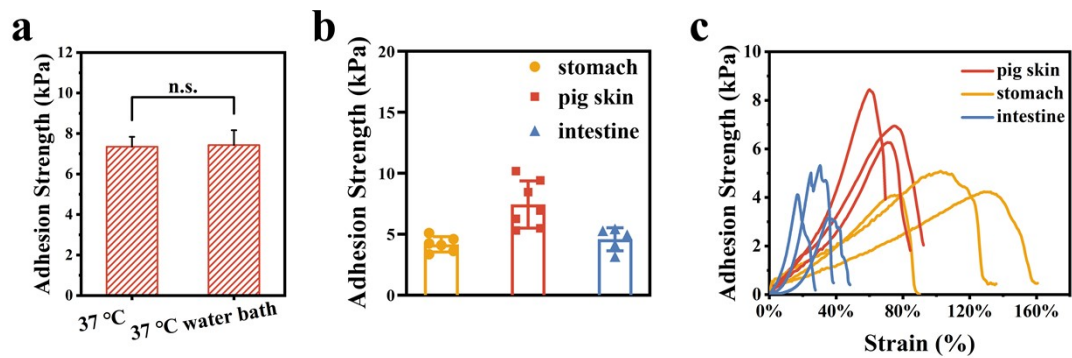


Fig. S4 (a) Adhesive strength of the GTPC hydrogel to pig skin in air and water at 37 °C. Adhesion strength (b) and lap shear curves (c) of GTPC hydrogel to different tissues.

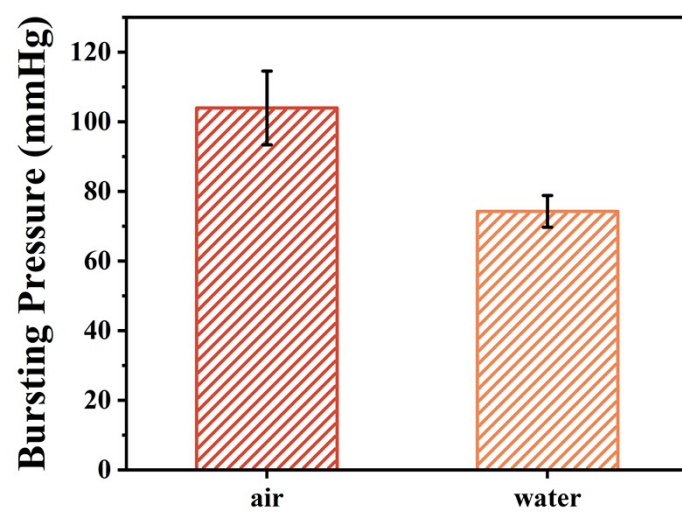


Fig. S5 Bursting pressure of the GTPC hydrogel to intestine tissue in air and water, respectively.



Fig. S6 Photographs of the asymmetric adhesion property of GTPC hydrogel.

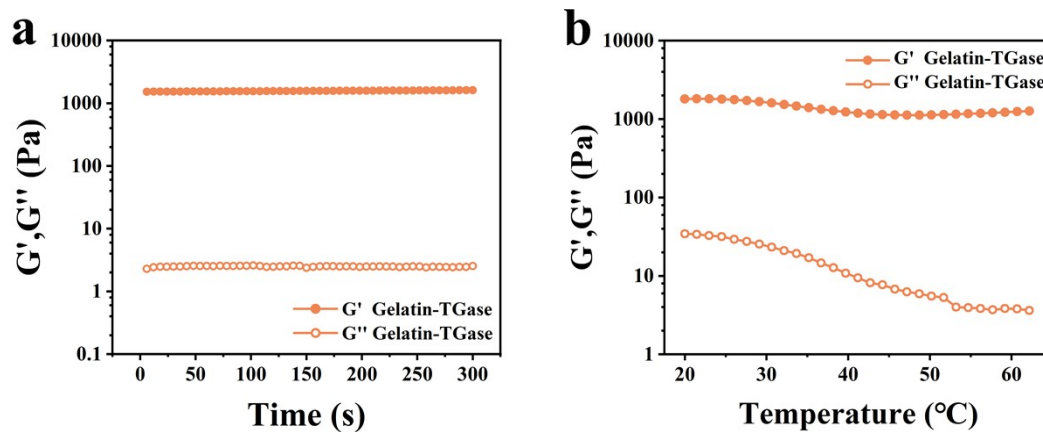


Fig. S7 (a) Time sweep rheological analysis to evaluate the stability of gelatin hydrogel crosslinked with TGase at 45 °C. (b) Temperature sweep rheological analysis to evaluate the stability of gelatin hydrogel crosslinked with TGase at different temperature.

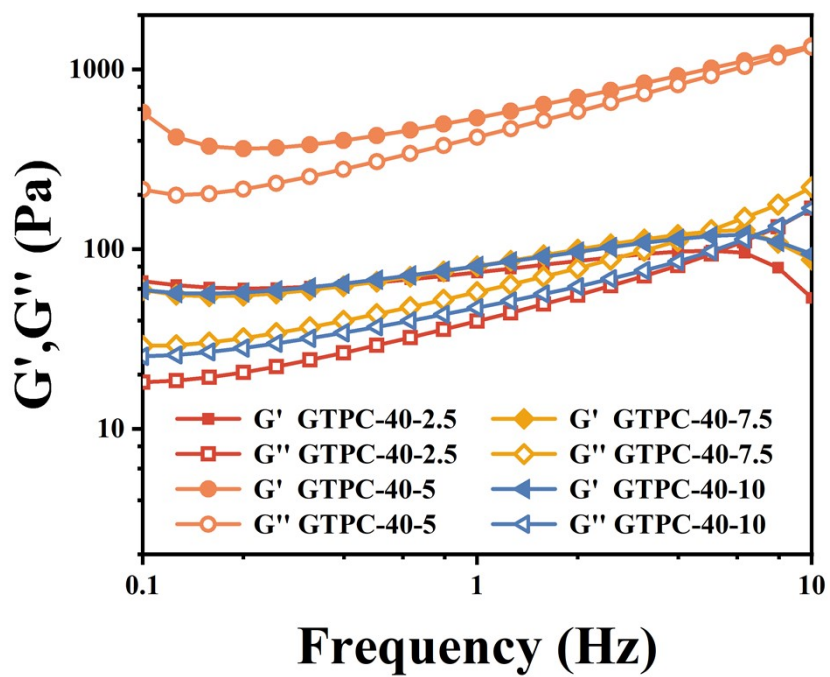


Fig. S8 Frequency sweep (37 °C) of GTPC hydrogels with different PC concentration.

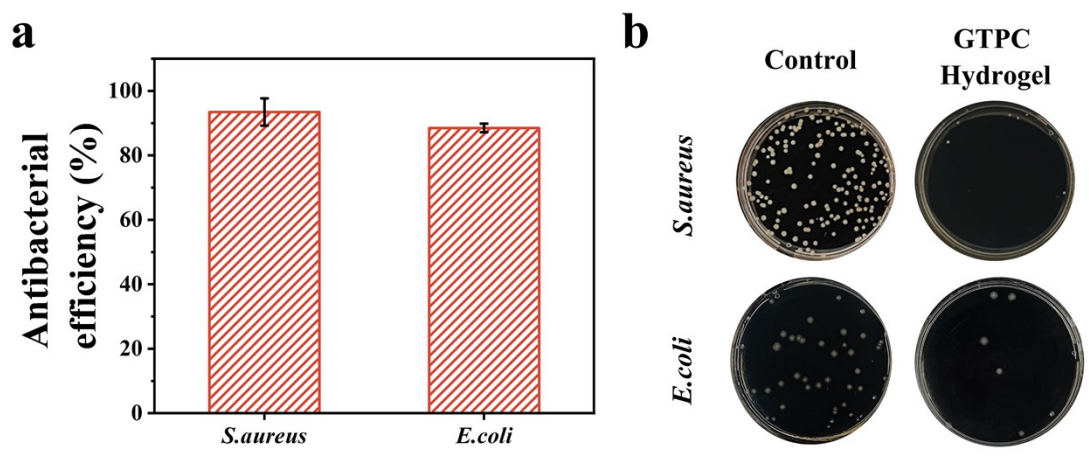


Fig. S9 (a) Antibacterial efficiency for *S. aureus* and *E. coli* of GTPC hydrogel.

(b) Images of bacterial cultures in control and experimental groups.

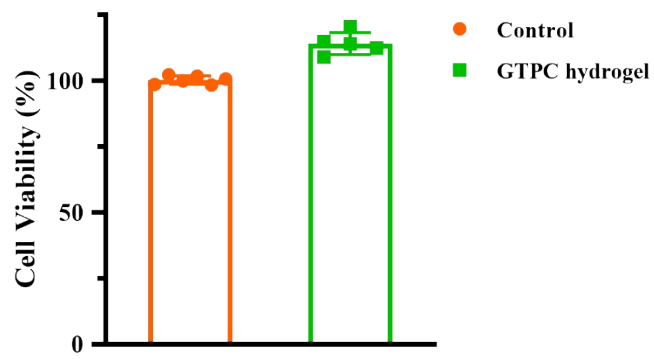


Fig. S10 In vitro cytocompatibility of the GTPC hydrogel.

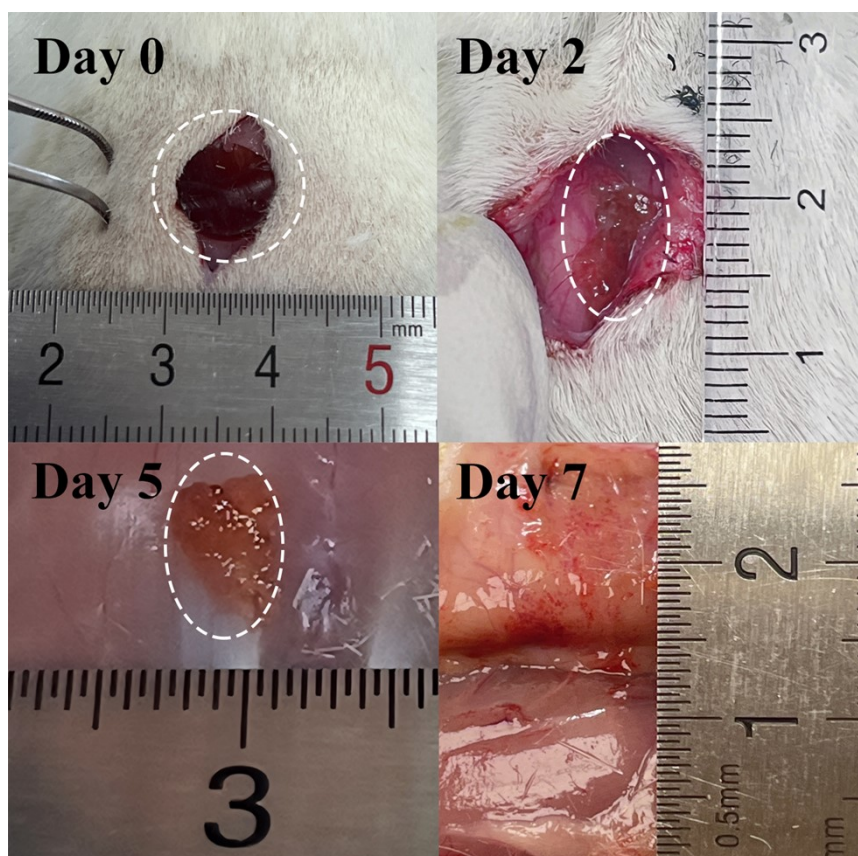


Fig. S11 Degradation of the GTPC hydrogels at different time points in vivo. White circle denotes the location of the hydrogel.

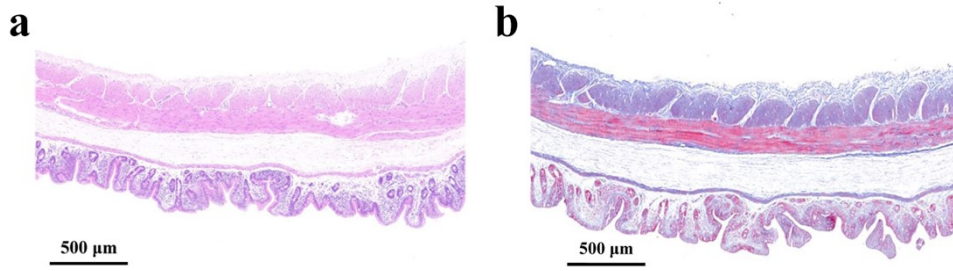


Fig. S12 (a) H&E and (b) Masson staining histological images of normal cecal wall.

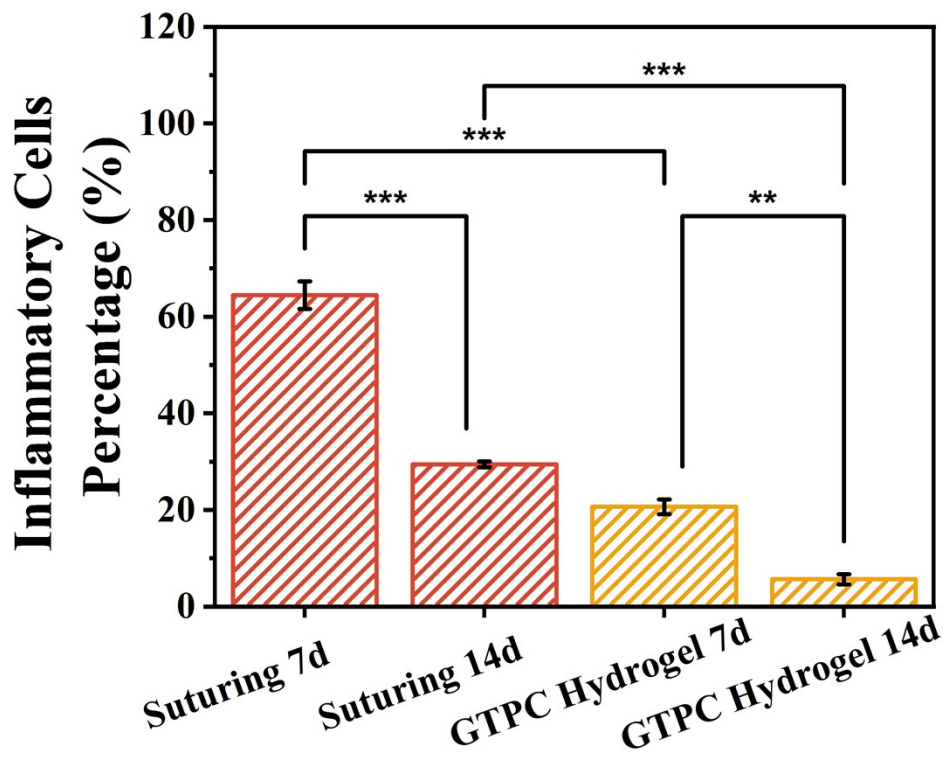


Fig. S13 Quantitative analysis of the percentage of inflammatory cells in all cells at the cecal damaged site after 7 or 14-day treatment using surgical suture or GTPC hydrogel (** $p < 0.01$, *** $p < 0.001$).

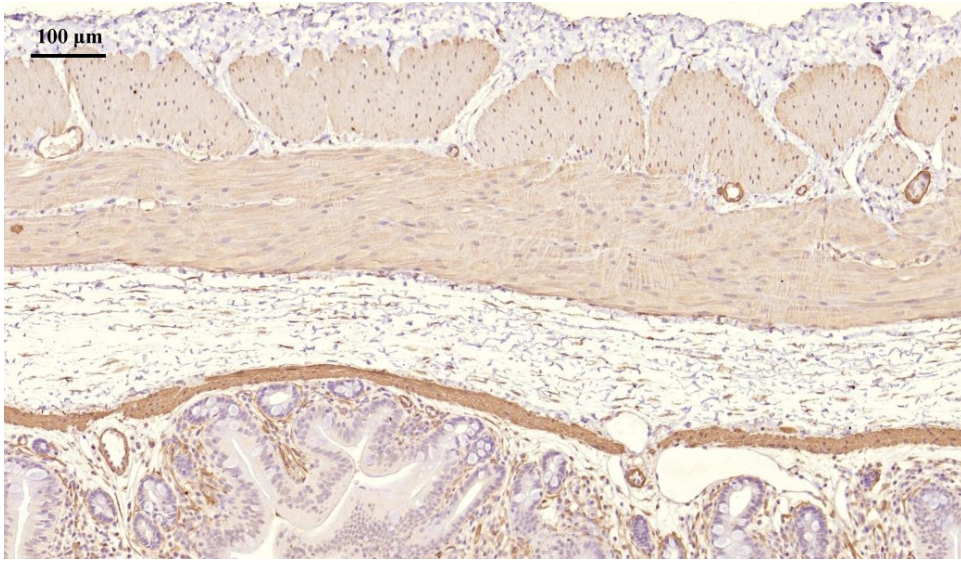


Fig. S14 α -SMA protein immunohistochemical staining image of normal cecal wall.